Egyptian Journal of Geology

https://egjg.journals.ekb.eg

Genetic constrains of uranium deposits associated with alkali metasomatism from the north Eastern Desert of Egypt: Gabal Abu Hamr and Gabal Gattar

Hicham M. Abdel Hamid

Nuclear Materials Authority, Cairo, Egypt

THE METASOMATITE uranium deposit is one of the significant uranium deposit categories world- wide, associating structurally-deformed rocks affected by metasomatic processes in a post-magmatic stage. U-mineralizations recorded along the contact zones at Gabal (G.) Abu Hamr, as well as, G. Gattar represents the unique discovered examples of the metasomatite U-deposits type in Egypt. Alkaline hydrothermal solutions arose at both sites during the youngest Red Sea-Gulf of Suez rifting extensional force, which affected Egypt since the Tertiary time along a NE- SW direction. These solutions generated a metasomatic zone between the arfvedsonite granite and the metavolcanics at G.Abu Hamr, and between the younger granite and the Hammamat sedimentary rocks (HSR) at G. Gattar. The residual melts, loaded with radioactive elements, are structurally controlled in both localities along the NNE-SSW direction. Primary and secondary U- and Mo-mineralizations were detected at the metasomatic zone of G. Abu Hamr, while only secondary U-mineralizations were recorded at the metasomatic zone at G. Gattar. Despite the difference in rock types in both localities, the mode of occurrence and genesis for both uranium mineralizations at the contact zones are quite very similar.

Keywords: Gabal Abu Hamr, Gabal Gattar, uranium, metasomatism, North Eastern Desert and Egypt.

1. Introduction

The Arabian Nubian Shield (ANS) represents the most extensive Gondwana-forming orogeny, which was generated by the closure of the Mozambique Ocean (Kusky et al. 2003; Jacobs & Thomas, 2004; Abu Sharib et al. 2019). The Red Sea rift valley separates the Nubian Shield, which crop out in the Eastern Desert of Egypt, Sudan, and Ethiopia, from its counterpart, the Arabian Shield, which is found in Saudi Arabia and Yemen (Fig.1a). The ANS is a vast tract of juvenile crust in northeast Africa and Arabia that originated during the Neoproterozoic East African orogenic cycle (c. 850–550 Ma) (Johnson et al., 2013 and Yeshanew, 2017). According to Stern (1994), the tectonic history of the ANS coincides with the break-up of Rodinia (~850 Ma) during the Cryogenian (850–635 Ma) and Ediacaran (635–541 Ma) periods. During the Early Cambrian time (~525 Ma), the ANS stabilized as a continental crust (Garfunkel, 1999; Robinson et al., 2014).

Several anorogenic within-plate granitic complexes intruded the Pan-African orogenic shield rocks of eastern Egypt, including G. Gharib (Abdel-Rahman and Martin, 1990a), G. El-Sibai (Abdel-Rahman and El-Kibbi, 2001), G. Abu Kharif and El-Dob (Abdel-Rahman, 2006 and Abdel Wanees, et al., 2021) and G. Abu Hamr (Abdel-Hamid, et al., 2019).

The Egyptian Eastern Desert (Fig. 1b) is subdivided into three terranes: the Northern (NED), Central (CED) and Southern (SED), based on rock types and their absolute ages in each one (Stern and Hedge, 1985). Post-orogenic felsic granite intrusions, Dokhan volcanics and molasse type sediments of the Hammamat Group are the main rock units in the NED. Metavolcanics, metasediments and diorite–granodiorite–trondhjemite intrusives are distributed in a few areas of the NED (Eliwa et al. 2014)

Egyptian granites have been subdivided into older and younger granites based on field and tectonic relationships, and geochronological studies (El-Sayed, 1998; Akaad & Abu El-Ela, 2002; El-Bialy &Hassen, 2012; Stern, 2018; Stern & Ali, 2020). The older granitoids, referred to gray or syn- to late-orogenic, low potassium calc-alkaline diorite, tonalite-granodiorite assemblages which crystallized during a Cryogenian orogenic stage (850–635 Ma).

The younger granites are post-orogenic, high potassium calc-alkaline, alkali feldspar granite, syenogranite, and monzogranite, crystallized during an Ediacaran orogenic stage (635–541 Ma).

Fifteen types of uranium deposits have been mentioned in the new IAEA classification scheme (OECD/NEA-IAEA, 2014). They are listed in order from deep primary magmatic, sedimentary and surficial deposits according to the geological cycle of Cuney (2010). One of these types is the metasomatites deposits. They are mainly confined to Precambrian

*Corresponding author e-mail: hichamel_hakim@hotmail.com
Received: 22/12/2024; Accepted: 06/01/2025
DOI: 10.21608/EGJG.2025.345866.1098

rocks affected by intense alkaline metasomatism of sodium or potassium series. The metasomatites are recoreded on the contacts of ancient shields where they form stock works controlled by ancient faults.

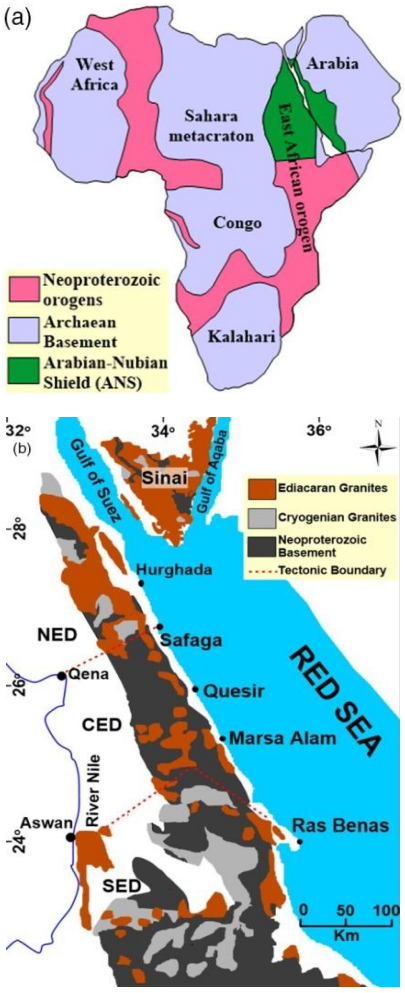

Fig. 1: (a) Geographical distribution of the East African Orogeny (EAO) in Africa and Arabia (Abu Sharib et al. 2019). (b) Distribution map of the Egyptian granites in the Eastern Desert and Sinai (El-Bialy, 2020).

In this type, uranium mineralization is structurally controlled and concentrated along and adjacent to faults associated with the metasomatism of the host rocks (Pownceby and Johnson, 2014).

Uranium deposits in sodium or in potassium metasomatites occur in Kirovograd Ore District, Ukraine, Beaverlodge (Canada), Itatiaia (Brazil), Jaduguda (India), and Kokchetav Massif (Kazakhstan) and Elkon Horst, the southern Yakutia, Russian Federation (Cuney et al., 2012). In Egypt, this metasomatite deposit was recorded only at G. Abu Hamr, and at G. Gattar.

The aim of this paper is to provide the essential mechanisms controlling the formation of the U-mineralizations of G. Abu Hamr and G. Gattar occurrences and the comparison between their origins. The investigated areas are located on the Red Sea coast in the Northern Eastern Desert (Fig.2).

The uranium mineralization occurs along the contact between the arfvedsonite granites and the metavolcanics at G. Abu Hamr; in contrast it occurs along the contact between Gattar granite and the Hammamat sedimentary rocks at G. Gattar.

These areas have been dealt with many authors. Among those authors; Mahdy et al. (1990), El Rakaiby and Shalaby (1992), ,Mahdy (1999) , El Kammar et al (2001) , Abdel-Hamid (2006), Abdel-Hamid (2009), Amin (2010), El Dabe (2010), Mahdy et al., (2013), El Sundoly (2016) and Waheeb (2021).

G. Gattar area contains two groups of uranium occurrences. The first group is called the ***"Intra-granitic"*** occurrences which bear the geological and alteration features of the vein-type deposits. The other group is called ***"Granite-Hammamat contact-related"*** occurrences which carry the geological and wall-rock alteration characters of contact metasomatic deposits. The studied zone in this paper belongs to the second groupe.

2. Methodology

A detailed field study, in addition to a of radiometric survey, was carried out along faultcontacts in both G. Abu Hamr and G. Gattar. The radiometric measurements carried out by using a Portable Gamma Ray Scintillometer Detector, model RS 320. The measurements of the radioactivity of the rocks was determined in terms of count per second (CPS), total uranium concentration (ppm), thorium concentration (ppm) and potassium percent (K %). The samples collected from the contact zones at G.Abu Hamr and G. Gattar were subjected to a separation technique to separate the light and heavy minerals using the heavy liquid (Bromoform Sp.Gr.= 2.82). The minerals were easily picked as individual minerals under the binocular microscope. At the laboratories of the Nuclear Materials Authority of Egypt, the picked minerals were identified and analyzed (semi-quantitative evaluation of their elemental composition) by using an Environmental Scanning Electron Microscope (ESEM) supported by an energy dispersive spectrometer (EDS) unit (model Philips XL 30 ESEM).

3. Geological Setting

G. Abu Hamr is located in the north Eastern Desert of Egypt. It consists of a series of granitic rocks belonging to the ANS developed during the Pan-African orogeny. An elongated peralkaline (arfvedsonite) granitic mass is intrudes the Precambrian country rocks (Fig.3). These mass trends NE-SW to ENE-WSW due to the fact that its intrusion was structurally controlled by a pre-existing fractures trending ENE-WSW (The same as the orientation of what so-called the Qena-Safaga shear zone). This arfvedsonite granite occurs a mountainous terrain, forming high-relief ridges and

multi-peaks. It is massive, medium to coarse-grained, highly fractured and well jointed (Fig.4). The granites range in color from white, pinkish-white to red. Quartz, aplite, jasperoid and black silica veins as well as basic dike surround these granitic rocks, which are completely free from the acidic dikes. The granitic pluton is cut by a major ENE-WSW right-lateral strike- slip fault on which hydrothermal solutions were emplaced causing the metasomatism of these granitic rocks (Abd El-Hamid, 2009).

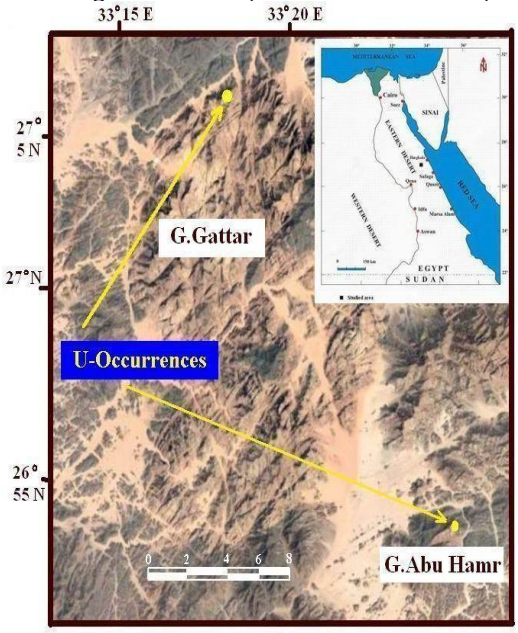

Fig. 2: Location map and landsat image of the G. Abu Hamr and G. Gattar areas and their related U-Occurrences.

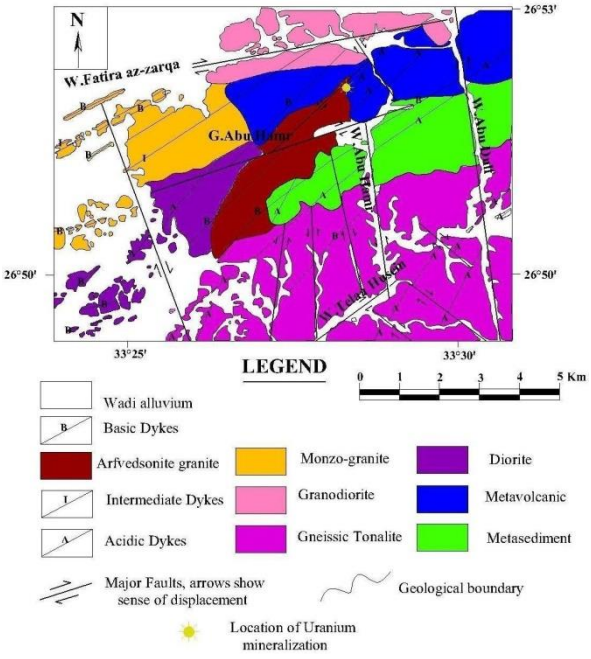

Fig. 3: Geological map of the G. Abu Hamr, North Eastern Desert, Egypt (Abd El-Hamid, 2009).

Fig. 4: Field photo showing G. Abu Hamr granite peaks as seen from W. Abu Hamr. Photo looking SE.

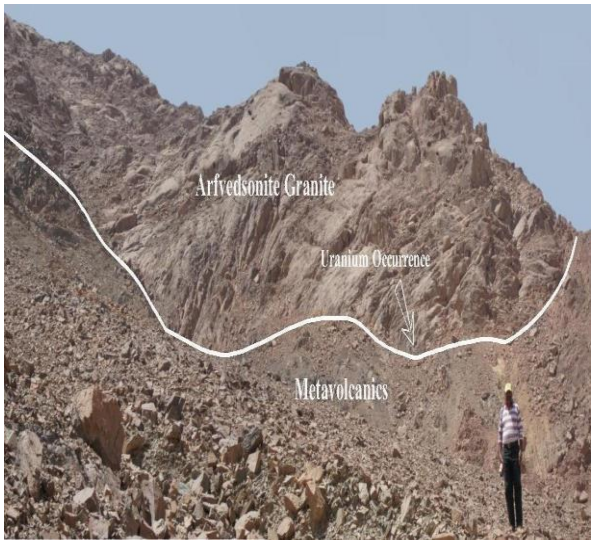

Fig. 5: Uranium occurrence along the contact between the arfvdesonite granite and metavolcanics. Photo looking E.

The arfvedsonite granite intruded the adjacent metavolcanic belt on a fault contact (Fig.5). Along this contact, U- and Mo- mineralizations were detected trending NNE-SSWto NE-SW with dips of about 77° to E (Fig.6).

The main characteristic alteration features detected on the contact zone at G. Abu Hamr are hematitization, epidotization, silicification, fluoritization and kaolinitization.

A trench was drilled with dimensions 2m x 1m (width) with 1m depth at the mineralized zone between the granite and the metavolcanics (Abd El-Hamid, 2019). On the surface, there are visible yellowish-green grains accompanied with high radiometric measurements, which are an indication of the uranium enrichment in this location. After drilling to 50 cm, two types of U minerals were found: the yellowish green grains and black ones. These two types indicate the presence of both primary and secondary uranium minerals. The radiometric

measurements increase with depth, especially in the NNE-SSW direction. This is the same trend of the fault contact between the arfvedsonite granite and the metavolcanics, which indicates that the mineralized solutions are mainly structurally controlled.

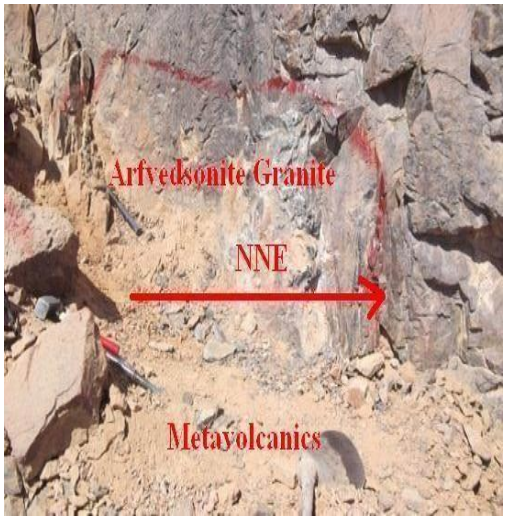

Fig. 6: Field photo showing the fault contact between the arfvedsonite granite and metavolcanics. Photo looking E.

G. Gattar is located in the northern domain of the Eastern Desert, which is considered a part of the Egyptian portion of the ANS, and it mainly comprises Pan-African rocks. It is dominantly composed of the younger alkali feldspar granite, with an exposure of the HSR of molasse-type (Fig.7). The younger granite of G. Gattar intrudes the Hammamat rocks with sharp intrusive contacts (Fig.8). The Hammamat rocks consist of alternating beds of graywackes and siltstones.

Along this contact, apophyses and offshoots of this granite invade into the HSR in the form of straight granite tongues. In addition, the granite contains xenoliths of the HSR (El Zalaky, 2002; Abdel Hamid, 2006).

At the contact zone between the HSR and the Gattar granitic intrusion were recorded some local reverse faults trending ENE- WSW (Shalaby, 1990).

Gattar granites are younger (~603 Ma) and have a typical A-type chemical characteristic. They are post-orogenic, emplaced at shallow levels characterized by high potassium calc-alkaline, alkali feldspar affinity (El Kammar et al. 2001; Mohamed and El-Sayed, 2008 and Moussa et al. 2008). The granitic rocks range in color from pink to reddish pink. Along faults and fractures intersections, the color is turned pale or reddish brown. They were invaded by basic dikes whereas the acidic ones cut the HSR rather than the G. Gattar granite. Many quartz veins and veinlets occur along the contact zone between the HSR and the G. Gattar granite. They cause a slight silicification of the host rock.

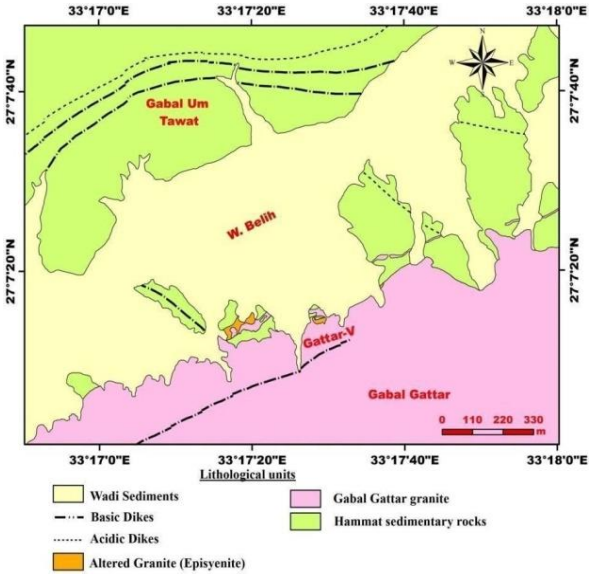

Fig. 7: Geological map of the U-occurrence at G. Gattar, North Eastern Desert, Egypt.

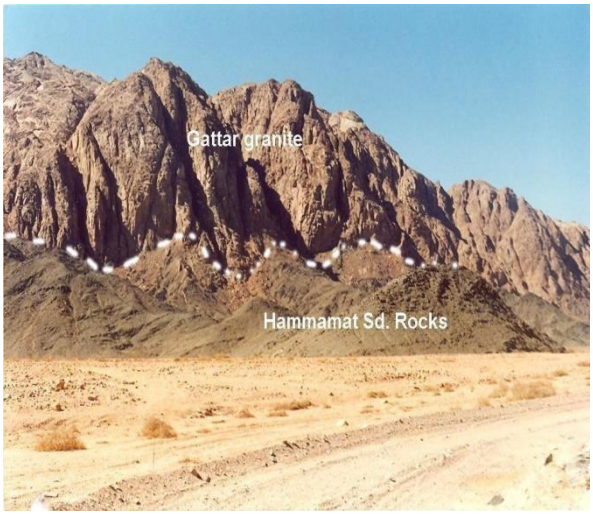

Fig. 8: Field photo showing sharp intrusive contact between G. Gattar and the HSR. Photo looking NE.

Along the contact zone between the alkali feldspar granites and the HSR, uranium mineralizations were recorded (Salman et al., 1986). These mineralizations have a yellow color and occur as small bundles with acicular needles, through the micro- fractures, foliations and joints of the HSR (Fig. 9). Waheeb and El Sundoly 2016 recorded that the uranium mineralizations are strongly controlled by the fault activities.

The uranium mineralizations were located in the footwall along a fault which strikes ENE–WSW to NE–SW and dips 73^{O} to SE. During the youngest NW–SE extension regime which affected the study area, this fault was reactivated from a compression thrust to a tensional diagonal normal and sinistral fault event (Waheeb and El Sundoly, op. cit.).

Some uranium mineralizations were recorded along tension joints associated with normal fault striking $N50^{O}E$ and dipping 85^{O} to SE.

Fig. 9: close up view showing the U-mineralizations staining the joints surfaces in the altered HSR of the uranium occurrence at G. Gattar.

At the contact zone in G. Gattar, the episyenitization process is a characteristic alteration feature of the granite, mostly accompanied with the existence of the uranium mineralization. The episyenitized granites occur as irregular bodies related to major faults and tension fracture zones reflecting a younger tension regime from the NW–SE direction. The studied rocks along this contact are characterized by a n intense fracturing and substantials alterations. Most of the visible uranium mineralizations were recorded at the bleached siltstones beds with scarce spots in the G. Gattar granite (Shalaby, 1996).

The subsequent fluids and hydrothermal solutions affecting the area cause many alteration features frequently pervasive along the contact zone. Strong hematitization, bleaching and fluoritization besides carbonatization, kaolinitization and manganese dendrites are the common alteration features associated with the HSR.

Episyenitization, hematitization, silicification, kaolinitization, chloritization and fluoritization besides the frequent presence of manganese dendrites are the commonest wall-rock alteration features manifested in the G. Gattar granite (Fig.10).

Fig. 10: Field photo showing the episyenitization of the Gattar granite in the uranium occurrence of G. Gattar. Photo looking E.

4. Mineralogy

4.1 G. ABU HAMR, the minerals identified at the mineralized zone can be grouped into:

a- Uranium minerals.
b- Molybdenum minerals.
c- Uranium-bearing minerals.
d- Gangue minerals.

a- Uranium minerals

The uranium minerals identified in the mineralized zone are classified mainly as primary and secondary minerals. The identified primary uranium mineral is **uraninite (UO_2)** (Fig.11a). It is formed in reducing environments and their changing to oxidation environments led to the formation of secondary uranophane (Fig.11b).

The secondary uranium minerals are represented by **uranophane** and **kasolite**. Uranophane is quite common as a secondary mineral, formed by the alteration of uraninite (Fig.11c), while kasolite is an uncommon mineral, and it is found also as the result of the oxidation of uraninite (Fig.11d).

b- Molybdenum minerals

The molybdenum minerals detected along the metasomatic zone of G. Abu Hamr are classified as pure Mo minerals (molybdenite and powellite) and Mo-U minerals.

Molybdenite is molybdenum disulfide MoS_2; it was identified through the ESEM analysis, sometimes it contains inclusions of Mo-U minerals (Fig.12a).

Powellite ($CaMoO_4$), it is an uncommon mineral, typically formed in oxidized zones as a pseudomorph after molybdenite (Fig.12b).

Two Mo-U minerals were identified in the location: **iriginite** and **tengchongite**.

In the oxidized zones of hydrothermal Mo - U deposits**, iriginite** is the most abundant secondary mineral. It has the formula $(UO_2)\ Mo_2O_7.\ 3H_2O$.

Tengchongite is also considered as a U-Mo mineral. It has the formula $Ca(UO_2)_6(MoO_4)_2O_5{\cdot}12H_2O$. Under the binocular microscope, it is difficult to differentiate between iriginite and tengchonite, but the ESEM was used to differentiate between them.

c- Uranium-bearing minerals

Zircon is the main accessory mineral in the mineralized zone of G. Abu Hamr (Abdel-Hamid et al., 2019). Ideal zircon remains stable in crustal and upper-mantle environments. Natural zircon crystals differ chemically and physically due to a time-dependent structural damage caused by the radioactive decay of U and Th and their daughter products. Zircon produces isostructural solid solutions with numerous orthosilicate and phosphate compounds, including hafnon ($HfSiO_4$), coffinite

($USiO_4$), thorite ($ThSiO_4$), and xenotime-(Y) (YPO_4) (Finch and Hanchar 2003). Such solid solutions are non-ideal, with substantial miscibility gaps (Ushakov et al. 1999).

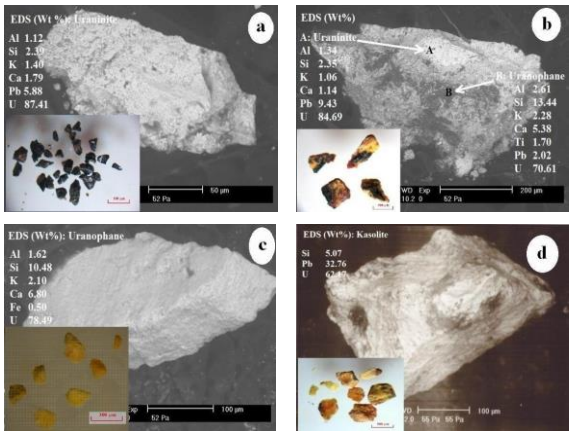

Fig. 11: BSE images, EDS analyses and separated grains fromG.Abu Hamr:

a- **Uraninite crystals.**

b- **Uraninite crystal (A) altered to secondary uranophane (B).**

c- **Uranophane crystals.**

d- **Kasolite crystals.**

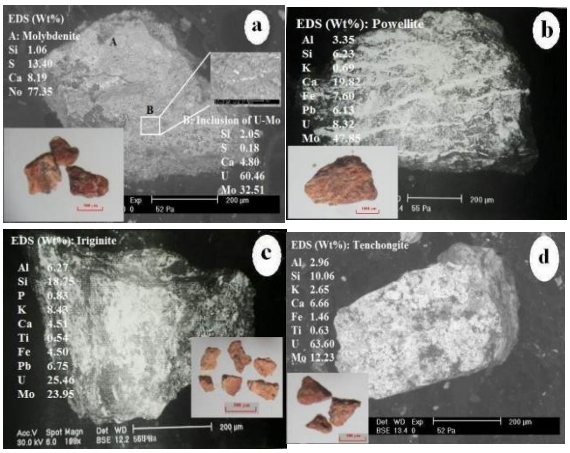

Fig. 12: BSE images, EDS analyses and separated grains from G. Abu Hamr:

a- Molybdenite crystal (A) with inclusion of U-Mo mineral (B).

b- Powellite crystals.

c- Iriginite crystals.

d- Tenchongite crystals.

During cooling, a zircon–coffinite solid solution, which crystallizes at a temperature near the coffinite's component solubility limit, becomes thermodynamically unstable. To reduce strain energy at low temperatures, this solid solution exsolve the coffinite component by replacing the U^{4+} cation for the ~ 16% smaller Zr^{4+} ion. After cooling, such a zircon solid solution exhibits structural strain and becomes metastable. This strain increases the surface reactivity and dissolving rate. Furthermore, the solubility of a non-ideal solid solution in a fluid is increased relative to the end- member (Lippmann, 1980).

Table (1) represents the EDS analyses results of eight zircon crystals separated from the arfvedsonite granite (samples A_1 to A_8) and eight zircon crystals separated from the mineralized shear zone (samples M_1 to M_8). These analyses justify the previous discussions. Some crystals represent solid solution of zircon-uranothorite (sample A_{6b}), zircon-xenotime (samples A_5 and A_8), metamict zircon and hydrothermal zircon. Also, allanite enriched in LREE and apatite are found to be included in zircon crystals (samples M_{6b} and A_{7b} respectively). The chemical variations in the composition of these zircon crystals indicate the different stages of alteration by metasomatism and hydrothermal alterations.

d- Gangue minerals

1- **Sulfides:** These minerals may be considered the leading cause of the reducing environments in the metasomatic zone. The main detected minerals were **pyrite** (FeS_2) and **galena** (PbS) (Figs.13a and b).

2- **Fluorite:** It is found in appreciable amounts as subhedral crystals that are characterized by vitreous luster and white streaks (Fig.13c). The majority of these crystals are generally violet with blue and deep blue shades (Fig.13d).

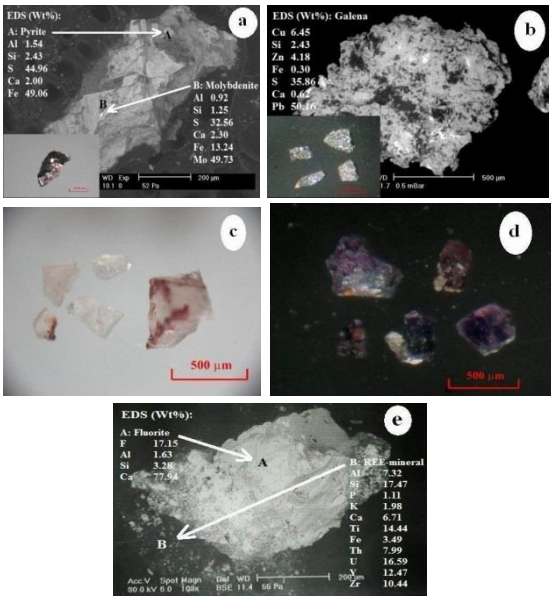

Fig. 13: BSE images, EDS analyses and separated grains from G. Abu Hamr:

a- Pyrite crystal (A) with inclusion of molybdenite mineral (B).

b- Galena crystals.

c- Colorless fluorite crystals.

d- Violet fluorite crystals.

e- Fluorite crystal (A) surrounded by an REE-bearing mineral (B).

The deep violet fluorite usually accompanies the

uranium mineralization, the color variation of the fluorite grains may be attributed to the fluoro-hydrocarbons or a radiation damage by the uranium components or a replacement of the Ca-group in the lattice by uranium or a combination of all (Abd El-Hamid, 2019). In some crystals there are inclusions of REE- bearing minerals, which was observed through the identification of fluorite mineral using the ESEM and EDS (Fig.13e).

4.2 G. GATTAR, the identified radioactive and associated minerals in the mineralized zone can be grouped into:

a- Uranuim minerals.
b- Gangue minerals.

a- Uranuim minerals.

The Uranium minerals identified are only secondary uranium minerals.
They are uranophane, beta-uranophane and Kasolite.
Uranophane Ca $(UO_2)_2$ SiO_3 $(OH)_2$*5(H_2O), is the commonest secondary uranium mineral present in the area. **Beta-uranophane** is a dimorph of the uranophane. In some chemical analyses, appreciable amounts of Fe, Pb, Al and K appear beside Ca, U and Si (Fig. 14a). Some uranophane crystals show a secondary enrichment of Fe attributed to Fe exchange for Ca in a later phase of mineralized fluids interaction.This is compatible with the results reported by Frondel (1958) and Heinrich (1958) for the chemical analyses of uranophane. The only uranyl silicate mineral observed is **kasolite** with major lead Pb (UO_2) SiO_4H_2O. Kasolite grains are relatively harder than the other secondary uranium minerals (Raslan, 1996). U, Pb, and Si are the major elements in kasolite, in addition to Ca, Al, K and Fe with fewer amounts (EDS analyses, Fig. 14b)).

b- Gangue minerals

1- **Fluorite**: It is found in appreciable amounts, and generally has violet with blue and deep blue shades (Fig.14c). The violet fluorite usually accompanies the uranium mineralization; the color may reach black especially in the composite fluorite and uranophane grains.
2- **Sulfides: galena, pyrite** and some other sulphide minerals (e.g: sphalerite and chalcopyrite) are identified at the contact zone of G. Gattar (Figs.14d&e).

5. Genesis of uranium mineralizations in the studied occurrences

From the previously mentioned information here, it was noticed that there is remarkable similarities between field characters and mineral assemblages in both localities, which may reflect that both occurrences have similar genetic origin.

5.1 G. Abu Hamr

As previously mentioned, G. Abu Hamr pluton is an elongated peralkaline granitic mass intrudes voluminous Pan-African country rocks along the NE to ENE shear zone (Qena-Safaga shear zone). Hydrothermal solutions caused the metasomatism of G. Abu Hamr arfvedsonite granite passed along the ENE-WSW major fault, which divided the pluton and led to the percolation of fluids rich in Zr, U, HREE through structures and their concentration along the tectonic contact between the granite and the metavolcanics (Abdel-Hamid et al., 2019).

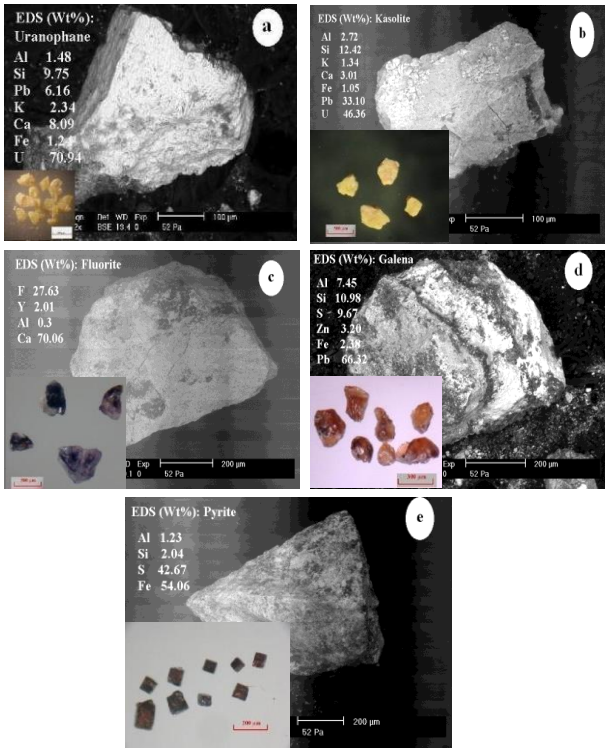

Fig. 14: BSE images, EDS analyses and separated grains from the metasomatic zone at G. Gattar:

a- Uranophane crystals.
b- Kasolite crystals.
c- Fluorite crystals.
d- Galena crystals.
e- Pyrite crystals.

Due to the presence of sulfides in the metavolcanics, the environment of crystallization was reducing, which favored the precipitation and crystallization of primary uranium and molybdenum minerals (uraninite, molybdenite) at depth. Due to the change in the oxygen fugacity, secondary uranium minerals and the oxidized types of molybdenum minerals (uranophane, kasolite, powellite) as well as Mo-U minerals such as iriginite and tengchonite, were formed near the surface. As the alkalinity decreases, the magmatic alkali zircon-silicate complexes were destructed and zircon crystals were formed. Finally, due to the percolation of meteoric waters along the shear zone the uranium mineralizations were partially leached, leading to the limited occurrence of uranium.

Table 1: EDS analyses for the zircon crystals separated from the arfvedsonite granite and the mineralized shear zone.

Wt.%	From the Arfvedsonite granite										From the Mineralized shear zone									
	A_1	A_2	A_3	A_4	A_5	A_6	A_{6b}	A_{7a}	A_{7b}	A_8	M_1	M_2	M_3	M_4	M_{5a}	M_{5b}	M_{6a}	M_{6b}	M_7	M_8
Zr	79.89	77.03	75.85	74.88	71.38	67.72	19.37	65.01	20.49	44.47	82.94	77.57	76.75	76.24	72.23	13.40	72.23	4.57	53.66	38.61
Si	16.33	18.34	17.07	19.71	15.35	17.65	13.07	20.86	5.27	13.00	14.46	21.54	20.50	20.69	19.55	15.79	20.94	28.32	26.12	13.03
Hf	1.91	2.85	2.28	2.64	3.12	3.40	2.00	2.28	–	2.32	1.87	0.89	2.16	1.28	3.44	0.87	5.34	1.08	7.11	1.33
Ca	1.15	0.42	0.84	1.08	0.59	0.99	2.17	0.99	55.82	5.86	0.73	–	0.58	1.19	3.52	4.08	2.79	11.21	2.28	5.15
Fe	0.72	0.59	0.63	1.00	0.46	5.99	5.43	6.51	–	4.01	–	–	–	0.64	1.26	8.22	3.90	38.62	2.32	1.14
U	–	–	1.15	–	–	1.46	8.90	–	–	1.31	–	–	–	–	–	0.63	–	3.18	2.46	39.02
Th	–	–	1.10	–	–	0.92	46.90	–	–	2.70	–	–	–	–	–	1.63	2.49	1.39	0.98	–
Al	–	0.77	1.09	0.70	–	1.19	2.15	1.86	–	0.92	–	–	–	–	–	–	–	1.63	3.01	1.38
Mg	–	–	–	–	–	–	–	1.48	–	–	–	–	–	–	–	–	–	2.23	1.53	–
K	–	–	–	–	–	0.68	–	1.02	–	–	–	–	–	–	–	–	0.34	7.24	0.34	0.34
Ti	–	–	–	–	–	–	–	–	–	–	–	–	–	–	–	–	–	0.73	–	–
P	–	–	–	–	–	–	–	–	18.41	–	–	–	–	–	–	1.36	–	–	–	–
Cl	–	–	–	–	–	–	–	–	–	–	–	–	–	–	–	–	–	0.22	0.29	–
Y	–	–	–	–	9.10	–	–	–	–	14.29	–	–	–	–	–	–	–	–	–	–
La	–	–	–	–	–	–	–	–	–	–	–	–	–	–	–	10.23	–	0.56	–	–
Ce	–	–	–	–	–	–	–	–	–	7.31	–	–	–	–	–	21.57	–	0.14	–	–
Pr	–	–	–	–	–	–	–	–	–	–	–	–	–	–	–	2.56	–	0.28	–	–
Nd	–	–	–	–	–	–	–	–	–	3.82	–	–	–	–	–	7.45	–	0.30	–	–
Sm	–	–	–	–	–	–	–	–	–	–	–	–	–	–	–	1.01	–	0.39	–	–
Total	100	100	100	100	100	100	100	100	100	100	100	100	100	100	100	100	100	100	100	100

- A_1; A_2; A_3; A_4; M_1; M_2; M_3; M_4 and M_{5a} pure zircons.
- A_{6b} solid solution between zircon and urano-thorite.
- M_{5b} and M_{6b} inclusion of allanite in the zircon.

A_5 and A_8 solid solution between zircon and xenotime.
A_{7b} inclusion of apatite in the zircon.
M_7 and M_8 are metamict zircons.

This interpretation is represented in Fig.15, which represents a model for the generation of the Abu Hamr granite and its U-Mo mineralizations.

5.2 G. Gattar

The formation of the uranium mineralizations in Gattar granites and the HSR has been a subject of heated debate during the last few decades. However, it is claimed that the mineralization of G. Gattar granite formed in stages. The Gattar pluton was formed in a within-plate tectonic setting from highly evolved peraluminous calc-alkaline magmas enriched in incompatible (LIL) and HFS elements (Roz, 1994; Nosseir, 1996; ; Shalaby,1996; Abdel- Monem et al., 1998; El-Sayed et al., 2003; El Feky, 2011; Shalaby et al., 2015).

An alkaline, oxidizing, uranium- enriched hydrothermal solution pervaded upwardly through the HSR and the G. Gattar granite, along the ENE-WSW and NE-SW fault regimes. These solutions developed metasomatic zones, associated with uranium, along the faults. In addition, U-mineralizations occur in the highly fractured and mylonitized zones along the contact as lensoidal bodies, where low-stress regions in the vicinity of a fault are favorable locations for fluid flow.

The changing in the physicochemical conditions of the hot fluids due to their mixing with meteoric water and the continuous interaction with wall rock caused the alteration of minerals such as dissolving quartz (episyenitization), albitization, sericitization, chloritization, muscovitization, hematitization and kaolinitization. Oxidation reactions have taken place by late weathering processes.

Uranium and other metallic elements were liberated from the structure of the primary accessory minerals due to silicification and the kaolinitization and concentrated in the mineralizing solutions. The deep circulating solutions were heated by the action of an elevated geothermal gradient from the radioactive decay of U, Th and K in granites (Birch, 1954; Fehn et al., 1978; Shrier and Parry, 1982; Min et al., 1999) as well as the intrusion of basic dikes (Roz, 1994). These dikes may have affected uranium mineralization and provided a possible redox boundary (chemical trap for the U-bearing solutions).

Also, the presence of sulfides (mainly pyrite) in the HSR is the major cause for the formation of the suitable reducing environments favorable for uranium crystallization. The hydrothermal solutions become mildly acidic due to the interaction with the host rock and passed through the shear zone. They leached uranium and other elements from the host rock during their percolation (Min et al., 1999). These fluids were rich in fluorine and CO_2 due to the abundance of fluorite veins and the regional occurrence of carbonates in the mineralized zone.

Mahdy (1999) mentioned that the main mineralizing fluids were carbonate-rich.

Fig.16 represents a model for the generation of the Gattar granite and its U mineralizations.

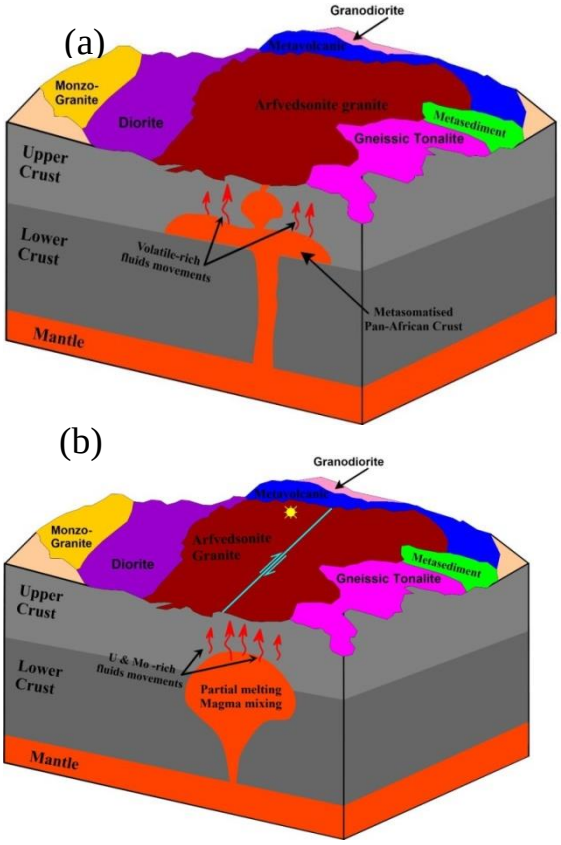

Fig. 15: Sketch model illustrating the genesis of the Abu Hamr granite and the U-Mo mineralization. (a) Abu Hamr granite was generated from metasomatised Pan-African crust. (b) The U-Mo mineralization along the granite-metavolcanic contact (yellow spot).

6. Conclusion

1- Uranium mineralizations at G. Abu Hamr and G. Gattar are unique recorded examples of metasomatite uranium deposits in Egypt.

2- Despite the different rock types in both localities (peralkaline granite and metavolcanics at G.Abu Hamr, and alkali granite and Hammamat sedimentary rocks at G. Gattar) the mode of occurrence and genesis for their uranium mineralizations at the contact zones are quite very similar.

3- In both localities, alkaline metasomatism took place at first by the ascending alkaline hydrothermal solutions following the same fault trend as a pathway (ENE-WSW direction). Then, the loaded mineralized solutions moved along the fault contact (NNE-SSW trend) till reached the suitable environment for the crystallization of the radioactive minerals.

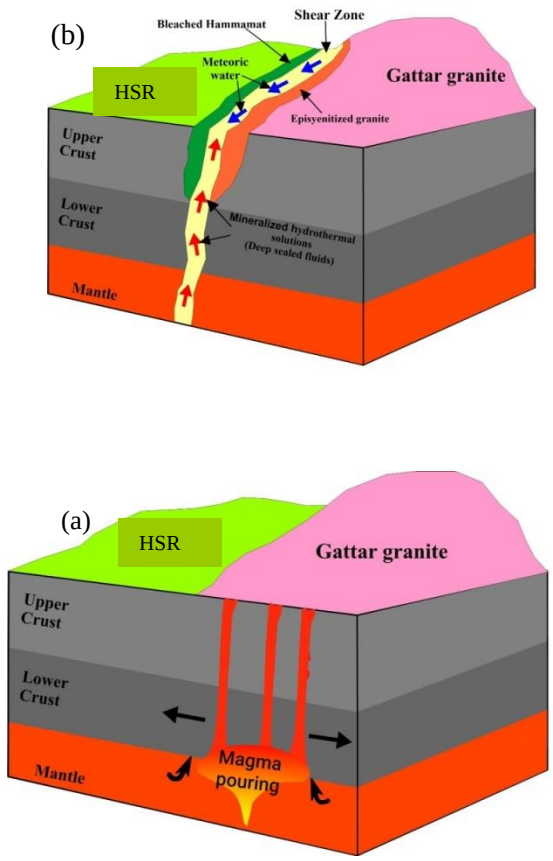

Fig. 16: Sketch model illustrating the genesis of the Gattar granite and the U- mineralization. (a) Gattar granite was generated from highly evolved magmas. (b) The U- mineralization along the granite-metavolcanic contact.

4- Both sites record almost the same mineral assemblages (uranophane, kasolite, fluorite and sulfides) but they differ at the contact zone in G. Abu Hamr where primary minerals were detected (uraninite and molybdenite). In contrast to the secondary mineralizations found at the contact zone in G. Gattar. In addition, only at G. Abu Hamr metasomatic zone, Mo-minerals were identified.

5- In spite of the previous discovery of primary uranium minerals (uraninite and pitchblende) by the geological team of the Egyptian Nuclear Materials Authority in the G. Gattar area, the lack of the primary uranium minerals at the contact zone with the HSR reflects that uranium may have been leached from granites and moved along structures to the contacts where suitable environments caused its crystallization in the form of secondary minerals.

6- The mineralizations in both occurrences are structurally controlled by the same tectonic event, which is the youngest major NE-SW extensional structural element of the Red Sea rifting. This may suggest that both mineralizations may have the same age of formation.

7- In G. Abu Hamr, despite the presence of both primary and secondary U-minerals, the discovered mineralization is on a small scale, which may indicate that uranium was later on leached from the contact.

Conflict of Interests: The author declares no conflict of interest.

Acknowledgements: The author would like to thank Prof. Dr. Abdel Hamid W. El Manawi, Faculty of Sciences, Cairo University and Prof. Dr. Hassan I. El Sundoly, Nuclear Materials Authority for their many insightful conversations as well as their critical evaluations and recommendations, which greatly enhanced the manuscript's quality.

7. References

Abdel-Hamid, A.A. (2006). Geologic factors controlling the radon emanation associated with uranium mineralizations along Wadi Belieh, North Eastern Desert, Egypt. M.Sc.Thesis, Geology Dept., Faculty of science, Benha Univ. 189p.

Abdel-Hamid, H. M. (2009). Geological and geochemical factors affecting the distribution of radioelements in Gabal Abu Hamr area, North Eastern Desert, Egypt, M. Sc. Thesis, Cairo Univ. 196.

Abdel-Hamid, H.M.; Abdel Kader, Z.M.; El Manawi, A.W., and Abdel Warith, A.(2019). Gabal Abu Hamr pluton: An example of A-type anorogenic peralkaline granites in Egypt. Egyptian Journal of Geology, v. 63, p. 291-305.

Abdel-Hamid, H.M.; Abdel Kader, Z.M.; Abdel Warith, A. and El Manawi, A.W., (2019). Mineralogical and geochemical studies on the genesis of the U- and Mo-mineralizations of Gabal Abu Hamr, North Eastern Desert, Egypt. Nuclear Sciences Journal, 8A, p. 207-229.

Abdel-Monem, A.; El-Amin, H.M.; El-Afandy, A.H.; Hussein, H.A. and Abdel-Aty, M.E., (1998). Petrological and geochemical characteristics of some younger granites bearing umineralization: Recognition criteria of uranium province in Egypt. Proc. Egypt. Acad. Sci., 48, 213-270.

Abdel-Rahman, A. M. (2006). Petrogenesis of anorogenic peralkaline granitic complexes from eastern Egypt. Mineral. Mag., 70(1), 27-50.

Abdel-Rahman, A. M. and El-Kibbi, M. M. (2001). Anorogenic magmatism: chemical evolution of the Mount El-Sibai A-type complex (Egypt), and implications for the origin of within-plate felsic magmas. Geol. Mag., 138(1), 67-85.

Abdel-Rahman, A. M. and Martin, R. F. (1990). The Mount Gharib A-type granite, Nubian shield: petrogenesis and role of metasomatism at the source. Contrib. Mineral. Petrol., 104, p. 173-183

Abdel Wanees, N. G.; El-Sayed, M. M.; Khalil, K. I. and Khamis, H. A., (2021). Petrogenesis of contrasting magmatic suites in the Abu Kharif area, Northern Eastern Desert, Egypt: implications for Pan-African crustal evolution and tungsten mineralization, Geological magazine 159 p. 441-467.

Abu Sharib, AS.; Maurice, AE.; Abd El-Rahman, YM. Sanislav, IV.; Schulz, B.; Bottros. R.; and Bakhit. BR., (2019). Neoproterozoic arc sedimentation, meta-morphism and collision: evidence from the northern tip of the Arabian- Nubian Shield and implication for the terminal collision between East and West Gondwana. Gondwana Research 66, p. 13–42.

Akaad, M.K. and Abu El-Ela, A.M., (2002). Geology of the basement rocks in the eastern half of the belt between latitudes 2530 and 2630N Central Eastern Desert, Egypt. Geological Survey of Egypt, Paper no. 78.

Amin, N.F. (2010). Surface and subsurface structural features controlling uranium mineralizations at granitic-Hammamat contact, Wadi Belieh, Northern Eastern Desert, Egypt. Ph.D. Thesis, Faculty of Science, Ain Shams University, 98p.

Birch, F., (1954). Heat from radioactivity. In: Fual, Henry (ed.): Nuclear Geology, New York, John Wiley, 148-174.

Cuney, M. (2010). Evolution of uranium fractionation processes through time: driving the secular variation of uranium deposit types. Econ. Geol. 105, p. 449-465.

Cuney, M., Emetz, A., Mercadier, J., Mykchaylov, V., Shunko, V. and Yuslenko, A. (2012). U deposits associated with sodium metasomatism from Central Ukraine: a review of some of the major deposits and genetic constraints. O.G.R. 44, p. 82-106.

El-Bialy, M.Z., (2020). Precambrian basement complex of Egypt. In The Geology of Egypt (eds Z Hamimi, A El-Barkooky, J Martínez Frias, F Harald & Y Abd El-Rahman), pp. 37–79. Cham: Springer Nature Switzerland.

El-Bialy, M.Z. and Hassen, I.S., (2012). The late Ediacaran (580–590 Ma) onset of anorogenic alkaline magmatism in the Arabian–Nubian Shield: Katherina A-type rhyolites of Gabal Ma'ain, Sinai, Egypt. Precambrian Research 216, 1–22.

El-Dabe M. M., (2010). Geology, geochemistry and radioactivity of some alkali feldspar granite intrusion in the Northern Eastern Desert, Egypt. Ph. D. Thesis, Assiut Univ., Egypt, 133 p.

Eliwa, H.H., Ramadan, E.M. and Nosair, A.M., (2014). Water/land use planning of Wadi El-Arish watershed, Central Sinai, Egypt using RS, GIS andWMStechniques. International Journal of Science and Engineering Research 5, 341–9.

El-Feky, M.G., (2011). Mineralogy, M-type tetrad effect and radioactivity of altered granites at the G. Abu Garadi shear zone, central Eastern Desert, Egypt. Chin. Jour. Geochem., 30,153-164.

El-Kammar, A.M., Salman, A.E., Shalaby, M.H., Mahdy, A.I., (2001). Geochemical and genetical constraints on rare metals mineralizations at the central Eastern Desert of Egypt. Chemical Journal 35, pp.117–135.

El Rakaiby, M.L. and Shalaby, M.H., (1992). Geology of Gabal Gattar batholith. Central Eastern Desert, Egypt. Int. J. Remote Sensing, Vol.13, pp. 2337 -2347.

El-Sayed, M.M., (1998). Tectonic setting and petrogenesis of the Kadabora pluton: a late Proterozoic anorogenic A-type younger granitoid in the Egyptian Shield. Chemie der Erde – Geochemistry 58, 38–63.

El-Sayed, M.M.; Shalaby, M.H. and Hassanen, M.A., (2003). Petrological and geochemical constrains on the tectonomagmatic evolution of the late Neoproterozoic granitoids suites in Gattar area, North Eastern Desert, Egypt. N . Jb. Miner. Abb., 178, 239 - 275.

El-Sundoly, H.I., (2016). Stress analysis and Radioactivity of Gabal Abu Hamr younger granites, Northern Eastern Desert, Egypt. Egypt. Jour. of Geol. 60: pp. 231-250.

El Zalaky, M. A., (2002). Interplay of plutonism, faulting and mineralization, Northern Gabal Qattar peripheral zone, North Eastern Desert, Egypt. M. Sc. Thesis, Benha Univ. Egypt, 178 pp.

Fehn, U.; Cathles, L.M. and Holland, H.D., (1978). Hydrothermal convection and uranium deposits in abnormally radioactive plutons. Econ. Geol., 73, 1556-1566.

Finch, R. J. and Hanchar, J. M., (2003). Structure and chemistry of zircon and zircon-group minerals. In: Hanchar JM, Hoskin PWO (eds) Zircon. Mineralogical Society of America Reviews in Mineralogy & Geochemistry 53, p. 1-25.

Frondel, C., (1958). Systematic mineralogy of uranium and thorium. U.S. Geol. Surv. Bull., 1064, p. 400 .

Garfunkel, Z., (1999). History and paleogeography during the Pan-African orogen to stable platform transition: reappraisal of the evidence from the Elat area and the northern Arabian-Nubian Shield. Israel J. Earth Sci. 48, 135–157.

Jacobs, J. and Thomas, RJ., (2004). Himalayan-type indenter-escape tectonics model for the southern part of the late Neoproterozoic-early Paleozoic East African Antarctic orogen. Geology 32, p.721–4.

Johnson, PR.; Halverson, GP.; Kusky, TM.; Stern, RJ. and Pease, V., (2013). Volcanosedimentary basins in the Arabian–Nubian shield: markers of repeated exhumation and denudation in a Neoproterozoic accretionary orogen. Geosciences 3, p.389–445.

Heinrich, E.W., (1958). Mineralogy and Geology of Radioactive Raw Materials. McGraw- Hill, New York, 621p.

Kusky TM.; Abdelsalam M.; Stern RJ and Tucker RD., (2003). Evolution of the East African and related orogens, and the assembly of Gondwana. Precambrian Research 123, p.81–5.

Lippmann, F. (1980). Phase diagrams depicting the aqueous solubility of binary mineral systems. Neues Jahrbuch für Mineralogie, Abhandlungen 139: p. 1-25.

Mahdy, A.A., (1999). Petrological and geochemical studies on the younger granites and Hammamat sediments at Gabal Gattar-5 uranium occurrence, Wadi Balih, North Easter Desert, Egypt. Ph.D. Thesis, Geology, Dept., Faculty of Science, Ain Shams Univ., 198 P.

Mahdy, M.A., Salman, A.B. and Mahmoud, A.H., (1990). Leaching studies on the uraniferous Hammamat sediments, Wadi Bali, Northern Estern Desert, Egypt, 14th Congress of Mining and Metallergy, Edinburgh Scotland, pp.229-235.

Mahdy, N.M, Shalaby, M.H., Helmy, H.M., Osman, A.F., El-Sawy, E.H., Abu Zeid, E.K., (2013).Trace and REE element geochemistry of fluorite and its relation to uranium mineralizations, Gabal Gattar Area, Northern Eastern Desert, Egypt. Arab Journal of Geoscience: DOI 10.1007/s12517-013-0933–2.

Mohamed, F.H., and El-Sayed, M.M., (2008). Post-orogenic and anorogenic A-type fluorite bearing

granitoids, Eastern Desert, Egypt: petrogenetic and geotectonic implications. Chem. Erde 68, 431–450.

Moussa, E.M.M., Stern, R.J., Manton, W.I., and Ali, K.A., (2008). SHRIMP zircon dating and Sm/Nd isotopic investigations of Neoproterozoic granitoids, Eastern Desert, Egypt. Precambr. Res. 160, 341–356.

Min, M.Z.; Luo, X.Z.; Du, G.S.; He, BA. And Campbell, A.R., (1999). Mineralogical and geochemical constraints on the genesis of the granite- hosted Huangao uranium deposit, SE China.Ore Geol. Rev., 14, 105-127.

Nossair, L.M., (1996). U-F bearing episyenitized "desilicified" granitic rocks of Gabal Gattar, North Eastern Desert, Egypt. Proc. Egypt. Acad. Sci., 46, 375-396.

OECD/NEA-IAEA (2014). Uranium 2013: resources, production and demand. A Joint Report by the OECD Nuclear Energy Agency and the IAEA. OECD, Paris.

Pownceby, M.I. and Johnson, C.,(2014). Geometallurgy of Australian uranium deposits. Ore Geol. Rev. 56: 25-44.

Raslan, M.F., (1996). Mineralogical and beneficiation studies for some radioactive granites along Wadi Balih, North Eastern Desert, Egypt. M.Sc. Thesis, Fac. Sci., Cairo Univ., Egypt.

Robinson, F.A.; Foden, J.D.; Collins, A.S. and Payne, J.L. (2014). Arabian Shield magmatic cycles and their relationship with Gondwana assembly: insights from zircon U-Pb and Hf isotopes. Earth Planet Sci. Lett. 408, p. 207–225

Roz, M.E., (1994). Geology and uranium mineralization of Gabal Gattar area, North Eastern Desert, Egypt. M.Sc. Thesis, Fac. Sci., Al-Azhar Univ, Egypt, 175p.

Salman, A.B.; El Aassy, I.E. and Shalaby, M.H., (1986). New occurrence of uranium mineralization in Gabal Gattar, north Eastern Desert, Egypt. Annals of Geological Survey of Egypt XVI, 31-34.

Shalaby, M. H., (1990). Uranium mineralization in the northern Gabal Qattar locality, Northern Eastern Desert. 7th Conf. Phanerozoic and Develop., Al Azhar Univ., Cairo, 3- 19 p.

Shalaby, M. H., (1996). Structural controls of uranium mineralization at Gabal Qattar, North Eastern Desert, Proc. Egypt. Acad Sci., 46: 521-536 p.

Shalaby, M.H.; Korany, E. and Mahdy, N.M., (2015). On the petrogenesis and evolution of U-rich granite: Insights from mineral chemistry studies of Gattar granite, North Eastern Desert, Egypt.Arab Jour. Geosci., 8, 3565-3585.

Shrier, T. and Parry, W.T., (1982). A hydrothermal model for the North Canning uranium deposit, Owl Creek Mountains, Wyoming. Econ. Geol., 77, 632-645.

Stern, RJ., (1994). Neoproterozoic (900–550 Ma) arc assembly and continental collision in the East African Orogen: implications for consolidation of Gondwana land. Annual Reviews of Earth and Planetary Science 22, p. 319–51.

Stern, R.J., (2018). Neoproterozoic formation and evolution of Eastern Desert continental crust: the importance of the infrastructure-superstructure transition. Journal of African Earth Sciences 18, 15–27.

Stern, R.J. and Ali, K.A., (2020). Crustal evolution of the Egyptian Precambrian rocks. In The Geology of Egypt, Regional Geology Reviews (eds Z Hamimi, A El-Barkooky, J Martínez Frias, F Harald & Y Abd El-Rahman), pp. 131–51. Cham: Springer Nature Switzerland.

Stern, R.J. and Hedge, C.E., (1985). Geochronologic and isotopic constraints on late Precambrian crustal evolution in the Eastern Desert of Egypt. American Journal of Science 285, 97–127

Ushakov, S.V., Gong. W., Yagovkina, M. M., Helean, K.B., Lutze, W. and Ewing RC (1999). Solid solution of Ce, U, and Th in zircon. Ceramic Transactions 93: p.357-363.

Waheeb , A. G., (2021). Resolved shear for the uranium mineralized fault contacts at Gabal Abu Hamr and Gabal Gattar, Northern Eastern Desert, Egypt. Annals Geol. Surv. Egypt. V. XXXVIII (2021), pp. 243 - 255

Waheeb, A. G. and El Sundoly, H. I., (2016). Structure roles for the localization of metasomatite uranium deposit type at Wadi Belih area, Northern Eastern Desert, Egyptian Journal of Petroleum 25: 201-214

Yeshanew, FG., (2017). Crustal evolution of the Arabian-Nubian Shield insights from zircon geochronology and Nd-Hf-O isotopes, Ph.D thesis, Stockholm University, Stockholm, Sweden, Published thesis.

القيود الجينية لرواسب اليورانيوم المصاحبة للتغير الكيميائي القلوي، شمال الصحراء الشرقية، مصر: جبل أبو همر وجبل جتار

هشام محمود عبدالحميد

هيئة المواد النووية، القاهرة، مصر

تعتبر تمعدنات اليورانيوم الموجودة على خط التماس فى كل من جبل أبو همر و جتار ٥ بجبل جتار المثالين الوحيدين لرواسب اليورانيوم المصاحبة للتغير الكيميائى القلوى بمصر. محاليل ساخنة قلوية تصاعدت فى كلا المكانين عبر اتجاة شمال شرق- جنوب غرب المرتبط بعملية فتح البحر الاحمر فى فترة الترشيرى بمصر. تسببت تلك المحاليل بتكوين منطقة تغير كيمائى على طول خط التماس بين صخور الجرانيت الارفزتونى و الصخور البركانية المتحولة بجبل أبو همر وأيضا على خط التماس بين صخور الجرانيت الجتارى وصخور الحمامات الرسوبية بجبل جتار. تحرك المحاليل المحملة بالعناصر المشعة متاثرة باتجاة شمال شمال شرق- جنوب جنوب غرب إلى أن حدث ترسيب لمعادن اليورانيوم معاددن المولبدن الاولية على طول خط التماس بمنطقة جبل أبو همر بينما يوجد فقط تمعادنات ثانوية لليورانيوم على خط تماس جبل جتار.